Durability Enhancement of Nafion® Fuel Cell Membranes Via In Situ Sol-Gel-Derived Titanium Dioxide Reinforcement

Yatin Patil, Kenneth A. Mauritz

School of Polymers and High Performance Materials, University of Southern Mississippi, 118 College Drive 10076, MS 39406, Hattiesburg

ABSTRACT: To improve durability of Nafion® membranes, samples were modified via an in situ sol-gel polymerization of titanium isopropoxide to generate titania quasi-networks in the polar domains. The incorporated titania reduced water uptake but equivalent weight was essentially unchanged. Fuel cell performance of the modified membrane was inferior to that of the unfilled membrane although these were considered as model studies with focus on mechanical durability. Mechanical analysis of contractile stress buildup during drying from a swollen state in samples clamped at constant length demonstrated considerable reinforcement of Nafion® by the titania structures. Tensile studies showed that at 80°C and 100% relative humidity the dimensional change of the composite membrane is one half and the initial modulus is three times higher than that of the unmodified membrane. During an open circuit voltage decay test the voltage decay rate for the modified membrane is 3.5 times lower than that of control Nafion®. Fluoride emission for the composite is at least an order of magnitude lower than that of the control Nafion® membrane indicating reduced chemical degradation. These model studies indicate that this in situ inorganic modification offers a way to enhance fuel cell membrane durability by reducing both physical and chemical degradation. © 2009 Wiley Periodicals, Inc. J Appl Polym Sci 113: 3269–3278, 2009

Key words: fuel cell; Nafion®; titania; sol-gel; mechanical durability

INTRODUCTION

Perfluorosulfonic acid ionomers are the most widely used solid electrolytes for polymer electrolyte membrane (PEM) fuel cells because they have a rather chemically inert hydrophobic backbone and perfluoroalkylether side chains with pendant sulfonic acid groups that have very low pK_a. The semi-crystalline nature of these ionomers provides a measure of mechanical strength while the long side chains assemble into a network of nanoscopic hydrophilic inverse micelle—type pockets with interconnecting channels that support proton conduction. Nafion® is currently the benchmark proton exchange membrane and considerable information on this polymer is available in a review article by Mauritz and Moore.[1]

One of the critical factors limiting the lifetime of a Nafion® PEM in a fuel cell is limited durability manifested by crack and pinhole formation which is attributed to the combined action of chemical and mechanical degradation.[2,3] Chemical degradation involves the attack of •OH radicals that issue from peroxide decomposition in the fuel cell environment and it is believed that the particular attack on Nafion® occurs on COOH groups at the chain ends,[4,5] although more recent experiments by Schiraldi et al. demonstrated that attack also occurs at the two ether oxygens on the side chains.[6] Nafion® membranes experience different water contents caused by humidity and temperature variations during fuel cell operation due to start-stop and changes in current density. There can also be spatial variation in water content due to non-uniform electrochemical reactions caused by uneven distribution of feed in gas distribution channels, localized hot spots and catalyst poisoning. Such water distribution gradients across mechanically constrained membrane electrode assemblies (MEA) can cause differential swelling that generates internal stresses. Water-swollen regions of low mechanical modulus adjacent to drier surrounding regions of higher modulus could be loci of membrane failure owing to differential swelling stresses.

The presence of hydrogen fluoride and small polymer chain fragments in the fuel cell effluent water is diagnostic of chemical degradation caused by attack of these hydroxyl radicals. The presence of both

hydrogen and oxygen on the catalyst surface due to fuel crossover results in partial reduction of oxygen to form hydrogen peroxide which on decomposition generates $^\bullet$OH radicals[7] that degrade the chain, as mentioned, reducing the average molecular weight and generating hydrogen fluoride. Fluoride emission rate (FER) is used to quantify Nafion[®] degradation. Degradation accelerates at high temperature and low humidity under the open circuit voltage (OCV) condition and this is used as a rapid test of membrane durability. The inter-connected ionic clusters in hydrated Nafion[®] provide paths of least resistance for gases to diffuse while the crystalline regions would be impermeable.

In concept, fuel crossover can be reduced if inert particles are placed along gas diffusion pathways, i.e., within the polar clusters. The obstacles generated by these particles would force gas molecules along tortuous pathways and reduce fuel crossover, thereby increasing membrane durability. Also, if these particles are interconnected they can form a load bearing network and provide mechanical reinforcement thereby minimizing both mechanical and chemical degradation. Porous Teflon[®] films have been used to reinforce cast thin Nafion[®] membranes. However, a hydrophobic support at a macroscopic level may not ensure dimensional stability during humidity change causing delamination.[8] Nano-scale interpenetrating reinforcements can provide dimensional stability against humidity changes and serve as fuel crossover impediments. Mauritz et al. were the first to report silicate particle growth and the incorporation of other metal oxide and organically modified silicate nanoparticles in Nafion[®] and discussed the use of these hybrid materials as useful permselective membranes.[9]

Using tetraethylorthosilicate as a silicate precursor, silica nanoparticles were shown, using SAXS, to form inside the hydrophilic ionic domains by sol-gel reactions. The in situ sol-gel technique is a site-targeted synthesis of such inorganic oxide inclusions as quasi-networks in the hydrophilic domains. In this work, we report formation of in situ grown titania nanostructures that reduce fuel crossover and improve membrane mechanical properties.

As the focus is on the aspect of mechanical durability, at this preliminary stage, no effort has been made as to optimize membrane performance in fuel cells although future research will address this.

EXPERIMENTAL

Materials

Titanium isopropoxide (Gelest) and 2,4-pentanedione (Acros organics) were used as received. Nafion[®] 112 membranes, received from E.I Dupont

Co. were cleaned and the procedure is described in the following section.

Composite membrane preparation

Nafion[®] 112 membranes were cleaned by boiling in 8M nitric acid for 2 h followed by boiling in deionized water twice for 2 h to leach out residuals. The membranes were then dried at 100°C under vacuum for 24 h. Titanium iso-propoxide was used as the sol-gel precursor monomer and to prevent its precipitation from reaction with atmospheric water 2, 4-pentanedione was added. A ratio of 0.4 : 1 for 2, 4-pentanedione-to-alkoxide monomer was maintained. The membrane was swollen in methanol for 24 h after which it was temporarily removed for ~ 30s during which time the sol-gel precursor monomer and 2, 4-pentanedione were added and stirred to form a homogeneous reaction solution. Then, the membrane was re-immersed for 15 min and after removal from the reaction mixture, followed by methanol wash, it was dried at 100°C for 16 h. After drying, the membrane was refluxed in 8M HNO_3 for 4 h followed by refluxing in deionized water twice for 1 h each. The membranes were then dried at 100°C for 24 h under vacuum.

Membrane electrode assembly (MEA) preparation

MEAs were prepared using Pt/C catalyst for both anode and cathode. Catalyst ink was prepared by mixing 30% HP Pt on Vulcan XC-72 (BASF Fuel Cell) with a 5 wt % Nafion[®] solution in a homogenizer for 10 min. Nafion[®] "solution" was prepared by mixing Nafion[®] films with a 1 : 1 ethanol-water mixture, by volume, in a high pressure reactor. The Nafion[®] content in the electrode was targeted to be 30%. The ink was then applied on a Teflon sheet by a doctor blade and dried. This was then decal transferred to the membrane in a Carver hot press under a pressure of 12 atm at 120°C for 5 min. The platinum loading in the electrode was gravimetrically estimated to be 0.41 ± 0.1 mg cm^{-2}. MEAs were assembled in a 5 cm^2 fuel cell hardware containing single serpentine flow fields. Two 275 μm thick Toray carbon paper (TGPH-090) were used as gas diffusion layers in the assembly. The assembly was sealed using two 225 μm thick Teflon gaskets and a torque of 4.5 N.m was applied on all the eight bolts of the assembly.

Inorganic uptake

The difference between the dried membrane weights following the sol-gel treatment and subsequent nitric acid/water cleaning is considered as the titania weight uptake.

Water uptake

Vacuum dried samples, after weighing for their initial weight, were immersed in deionized water for 24 h. The samples were taken out of water and blotted dry and weighed to determine water uptake.

Equivalent weight (EW) measurement

Vacuum dried membranes, after weighing for initial weights, were added to a flask containing deionized water and soaked for 24 h. To neutralize the acidic groups, a known excess of 0.01N standard sodium hydroxide solution was added to the flasks and stirred for 3 h. Excess sodium hydroxide was measured by titrating against 0.01N standard acetic acid solution using phenolphthalein indicator. EW weight was calculated by dividing number of moles of sodium hydroxide consumed by the sample into its dry weight.

Thermal analysis

Thermal degradation stability, under nitrogen, of the control and composite membranes was analyzed using a TA Q50 Thermogravimetric Analyzer. The samples were heated from room temperature to 800°C at 10°C/min.

FTIR analysis

The nature and extent of chemical bonding in the in situ-grown titanate nanostructures was investigated by FTIR/ATR spectroscopy using a Bruker Equinox 55 instrument. Samples were too thick (50–60 µm) for beam transmission; hence, the ATR mode was used, being aware that the immediate subsurface region ($\sim$ 1 µm) is interrogated and the degree to which the spectra are characteristic of bulk must be established independently. Samples were stored under vacuum at room temperature to minimize moisture gain although the presence of slight water cannot be ruled out. Each spectrum represents an average of 10, 5 on each side of the membrane collected at different locations. Spectra were baseline corrected and smoothed. The spectra were truncated below 530 cm^{-1} due to considerable noise at lower wavenumbers.

Mechanical analysis

Mechanical properties of membranes at 80°C and 100% relative humidity were tested using an MTS Alliance RT/10 tensile setup equipped with a 100N load cell. A custom design environmental chamber and a sparger were built to control chamber temperature and humidity. Eighteen millimeters wide samples were used for all the tensile experiments.

Electrical impedance measurements

Membrane proton conductivity was measured using a four point probe configuration in a Bekktech conductivity cell (BT-102). For uniform water content in the membrane, the cell along with the sample was immersed in deionized water. Impedance was measured in the frequency range 500 Hz to 1 MHz using an HP 4192 LF impedance analyzer. The Z′ intercept from Nyquist plots was taken, in the usual way, as the membrane resistance to compute conductivity.

Fuel cell performance and FER analysis

Polarization (voltage-current) curves were obtained at 80°C with 100% and 50% anode and cathode relative humidity, respectively. Prior to obtaining polarization curves, the membranes were conditioned for 6 h at 0.6 volts. Ultra high pure H$_2$ (0.2 cc/min) and ultra high pure O$_2$ (0.5 cc/min) gases were used. The voltage was scanned from the open circuit condition to 0.2 V.

To test durability and fuel crossover of the membranes, MEAs were tested under open cell voltage (OCV) conditions at 90°C and 30% relative humidity. Ultra high pure hydrogen (0.2 cc/min) and ultra high pure oxygen (0.3 cc/min) gases were used. The test was performed for 20 h and the anode and cathode effluent was independently collected in cold traps. Before the test, cold traps and the exhaust pipes were thoroughly washed to ensure no fluoride contaminants present. FER from the effluent was measured using a fluoride ion selective electrode (Metler Toledo DC219-F). Before FER measurements the electrode was calibrated for a 0.1–5 ppm range using fluoride standard solutions.

RESULTS AND DISCUSSION

Inorganic weight uptake

Titania weight uptake for the composite membrane used for all tests was gravimetrically measured to be 20%. The Nafion® control sample lost 3% of its initial weight, assumedly because low molecular weight fragments leached out of the membrane in alcohol solution during membrane swelling.

Water uptake and equivalent weight (EW)

The average value of the water uptake and EW of Nafion® and Nafion®/titania over three samples each is shown in Table I. Water uptake and EW of the Nafion®/titania composite membrane were calculated with respect to the Nafion® fraction (0.8) in

TABLE I
Equilibrium Water Uptake and Measured EW for
Nafion® and Nafion®/Titania Composite Membranes

	Nafion®/titania	Nafion®
Water uptake (weight%)	13.6 ± 2.1	22.3 ± 2.0
EW (g/mol)	1143 ± 20	1152 ± 37

the membrane. By this measure, water uptake of the composite membrane was 40% lower than that of the unfilled Nafion® membrane. For unfilled Nafion® the water uptake is distributed throughout the entire volume but for the composite membrane the titania structures occupy a considerable amount of space as well as reinforce the polymer (limiting swelling), thereby reducing the percent by weight. It might also be thought that titania particles inserted into the polar clusters simply block the entry of water molecules in these domains. However, the equivalent weights of Nafion® and Nafion®/titania are very close to 1100 g/mole, to within measurement error. This important fact indicates that incorporated sol-gel-derived titania quasi-networks have not altered the effective concentration of acidic groups that are essential for proton transport.

FTIR-ATR analysis

In our previous studies of Nafion®/silicate nanocomposite membranes, FTIR-ATR difference spectra were extracted to enhance the characteristic bands of the inorganic component.[10] In practice, the spectrum of the unmodified polymer is subtracted from that of the modified polymer so that obscuring polymer bands are eliminated or at least diminished. Here, the C—F stretching band at 1200 cm^{-1} was used as an internal standard to scale the absorbance of both spectra the same so that meaningful subtraction can be performed. The uniform-scaled ATR spectra for Nafion®/titania and unmodified Nafion® are shown in Figure 1. However, the difference technique does not work well for this sample as the Nafion® spectrum has higher absorbance than that of Nafion®/titania. Therefore, the direct spectra of each are inspected on the same scale. The band assignments for Nafion® and titanates are according to those of Falk[11] and Siuzdak et al.,[12] respectively.

When the membrane is introduced into the sol-gel reaction monomer solution, titanium iso-propoxide reacts very rapidly. The absorbance of all polymer bands can be expected to be diminished by virtue of having lower concentration because the inorganic component occupies part of the volume. This dilution effect, in fact, is seen across the spectral range in Figure 1.

Beginning at the high wavenumber region, there is the band for asymmetric S—O stretching in SO_3^-

groups. The maxima for the modified and unmodified samples coincide, but it is significant that the band width has not changed with inorganic modification. The unaltered band width can be interpreted as being due to an unchanged distribution of molecular environment around the sulfonate groups despite the inorganic incorporation. On the low wavenumber side of the SO_3^- peak is a strong CF_2—CF_2 band whose position is essentially invariant with inorganic modification. Continuing to lower wavenumbers, there is the symmetric stretching peak of the SO_3^- group whose wavenumber and profile does not change with inorganic modification. The wavenumber invariance of both sulfonate peak vibrations might indicate that the titanate phase does not interact with these groups as the S—O bond polarization does not seem to change as it might through inductive effects. This is in harmony with the unchanging equivalent weight, i.e., with titanate uptake, as discussed above.

The doublet at around 980–960 cm^{-1} is due to the two ether groups in the long side chains. The lower wavenumber component absorbance becomes of lesser absorbance relative to the high wavenumber component. This could indicate interactions of titanate structures with the two oxygens, both of which have hydrogen bonding capability.

Ti—O—Ti stretching vibrations are seen in a band at ∼ 700 cm^{-1}. This band is evidence of successful condensation reactions required for particle formation and the low peak height-to-peak width ratio indicates a broad distribution in the environment (mainly in the form of varying degrees of Ti atom coordination about bonded TiO_4 tetrahedra) about these vibrating groups. There is a CF_2—CF_2 band in this location, the absorbance which, of course, must

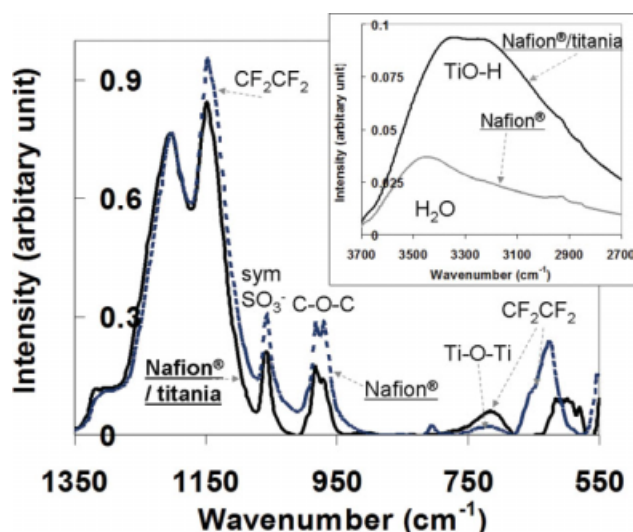**Figure 1** FTIR-ATR spectra of Nafion® and Nafion®/titania composite membranes.

account for part of the strength of the Ti—O—Ti band in the unsubtracted spectrum. The Ti—O—Ti band is not to be confused with the CF_2—CF_2 band because the composite band is of greater, rather than less than the absorbance associated with the CF_2—CF_2 band.

The inset in this figure shows absorbance in the region of the O—H stretching vibration for both the control and titania-modified Nafion®. Unmodified Nafion® shows a broad band that is likely due to water that exists in a large number of hydrogen bonding states. The Nafion®/titania sample also has a broad band in this region that can be ascribed to water molecules that hydrate accessible uncondensed TiOH groups as well as to Ti(O—H) stretching vibrations.

In summary, while there does not seem to be significant interactions between the SO_3^- groups and the inserted titanate structure, the ether groups, which are closer to the main chain, are affected. However, the CF_2 wagging peak at 628 cm^{-1} has disappeared and new broad peaks in the range of 640–570 cm^{-1} and 690–780 cm^{-1} have emerged. These new peaks could be due to Ti—O—Ti bonds. Mauritz and Jones[13] reported a strong broad peak in the range 400–660 cm^{-1} for Ti—O—Ti bond groups formed by sol-gel reactions of tetraethyltitanate in poly(n-butyl methacrylate). Also, oligomers of condensed tetrabutyltitanate have peaks at 820 cm^{-1} and 763 cm^{-1} due to Ti—O—Ti bonds. The Ti(0-R) vibration for uncondensed titanium iso-propoxide is located at 1005, 950 cm^{-1} as cited by Bradley et al.[14] These peaks are not expected because the sample was thoroughly refluxed with acid and water. In short, the FTIR analysis indicates successful titania network formation but with significant uncondensed non-interacting Ti—OH groups.

Thermal analysis

Weight loss and derivative curves for the Nafion® and Nafion®/titania membrane are shown in Figure 2. As reported by Samms et al. there are three derivative weight loss peaks for Nafion® around 50–250°C, 250–400°C, and 400–570°C. Samms et. al.[15] and Wilkie et. al.[16] reported that the initial weight loss is due to residual water. The next peak involves loss of the ionic functionality by evidence of sulfur dioxide and the final peak involves a side chain degradation shoulder followed by main chain degradation.

For the Nafion®/titania membrane we see the initial water weight loss. It can be seen here, as well, that the water uptake of the composite membrane is lower than that of Nafion®. A sharp weight loss derivative peak associated with loss of ionic functionality is observed in the range of 280–350°C. Not only
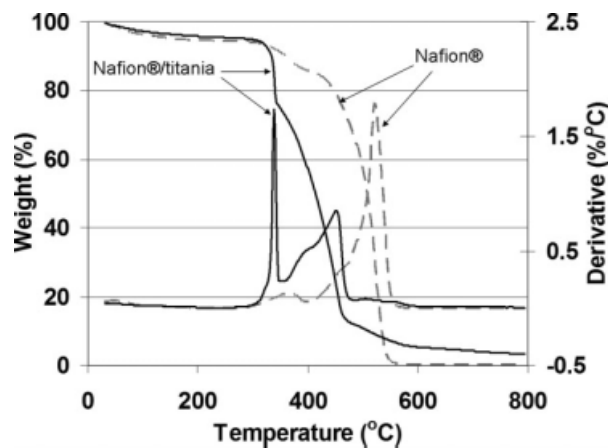

Figure 2 TGA and derivative curves for Nafion® and Nafion®/titania membranes.

does this occur very sharply but at a lower temperature than that of unmodified Nafion®. The next, bimodal, weight loss derivative peak from 364 to 470°C can be assigned to the loss of side and main chains. Again, this occurs at lower temperature than that of unmodified Nafion® and suggests that the presence of titania reduces Nafion®'s elevated temperature thermal stability. A very small broad peak around 470–600°C could be due to loss of moisture during condensation of surface TiOH groups. In short, the thermal stability of the composite membrane is less at elevated temperature although it will be seen that its stability at fuel cell operating temperature is comparable to that of Nafion®.

Mechanical properties

After mounting, the samples were conditioned for 2 h with a 100% relative humidity (RH) nitrogen stream supplied at a flow rate 300 ml/min. After such conditioning, the membrane swells due to water uptake, and to hold the sample to its extended swollen length, the crosshead position was slowly adjusted until a tension of 0.1N was detected by the load cell. The crosshead position was then locked and the 100% RH nitrogen stream was switched to dry nitrogen at the same flow rate (300 ml/min). The temperature of the dry nitrogen stream was the same as that of the humidified nitrogen stream and the chamber temperature was maintained at 80°C. This change of circulating gas stream caused the membrane to lose water and the sample attempted to regain its un-swollen length except that the clamps were locked at the swollen length position and the sample consequently exerted a contractile force. These resistive forces were monitored for 2 h after the humidity drop. Figure 3 shows the stresses developed for two Nafion® and two Nafion®/titania composite membranes measured for 2 h after the humidity drop.
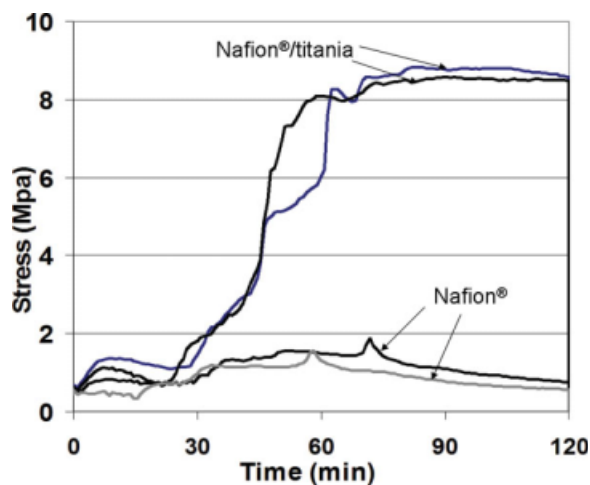
Figure 3 Stress response to humidity change from 100% to 0% at 80°C for H$^+$ Nafion® and a Nafion®/titania composite membranes.

The stress-time profiles developed for the two control Nafion® samples reach peak values at around 58 and 71 min, and then drop. The peak stress values for the two samples were 1.56 MPa and 1.89 MPa, respectively. The stresses in these samples do not peak at the same time as the rate of water loss by the samples could be different due to water condensation in the chamber or minor material differences. Nonetheless, the stress profiles for both samples are similar. Both samples yield after reaching a critical stress. Due to the low modulus and lack of cross-linking or reinforcement in this unfilled membrane, it is unable to withstand the contractile stress developed and yields likely through constant chain slippage through chain entanglements that limit the stress from increasing. In terms of viscoelastic theory, this could be considered as a viscosity-dominated process somewhat as discussed for the terminal region of creep compliance curves, or as a stress relaxation experiment in reverse.[17]

In case of the composite membrane, a different mechanical response is observed wherein the membrane resists the dimensional constraint. For both composite membranes, at ∼ 70 min the stress reaches peak values of 8.4 and 8.6 MPa and remains fairly constant during the timeframe of the experiments. It can be concluded from this test that the in situ grown titanium oxide quasi-networks provide good membrane reinforcement and prevent it from yielding due to humidity change. If, as is likely, chain slippage is involved in failure of this sort, then it can be imagined that the inorganic inclusions anchor the chains, thereby restricting their motion through entanglements. This quality could be beneficial for fuel cell membranes in the situation of clamped MEAs at the intersection of lands and grooves of a gas distribution plate that experience

periodic stresses due to humidity changes. Without such reinforcement, the unmodified membrane will experience structural and mechanical hysteresis such that swelling fatigue may eventually cause local yielding which can lead to cracking and ultimate failure.

Tensile stress-strain curves for four samples each of Nafion® and Nafion®/titania membranes at 80°C and 100% relative humidity are shown in Figure 4(a) and (b). The four curves are for the same sample and were randomly selected from different locations in the membrane. The samples after conditioning for 2 h with a 100% relative humidity nitrogen stream were stretched at a rate of 5 mm/min. The stress rise does not start at the origin so that the curves are displaced along the strain axis. The reason for this is that as the sample expands due to water uptake during conditioning the load cell does not register force until the sample reaches its natural length. The
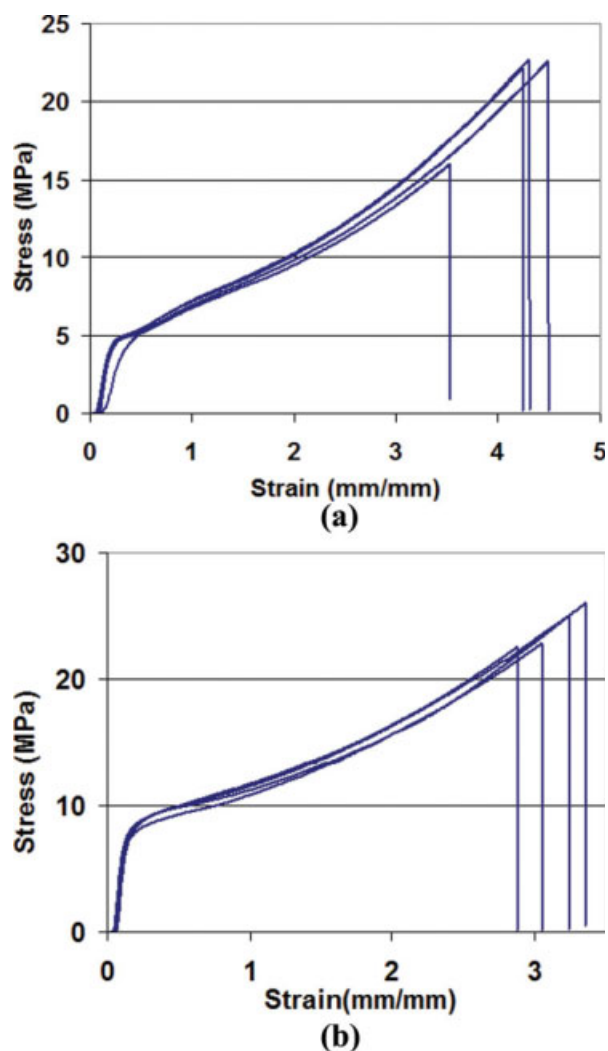

Figure 4 Tensile-stress strain curves at 80°C and 100% relative humidity (a) Nafion® and (b) Nafion®/titania composite membranes.
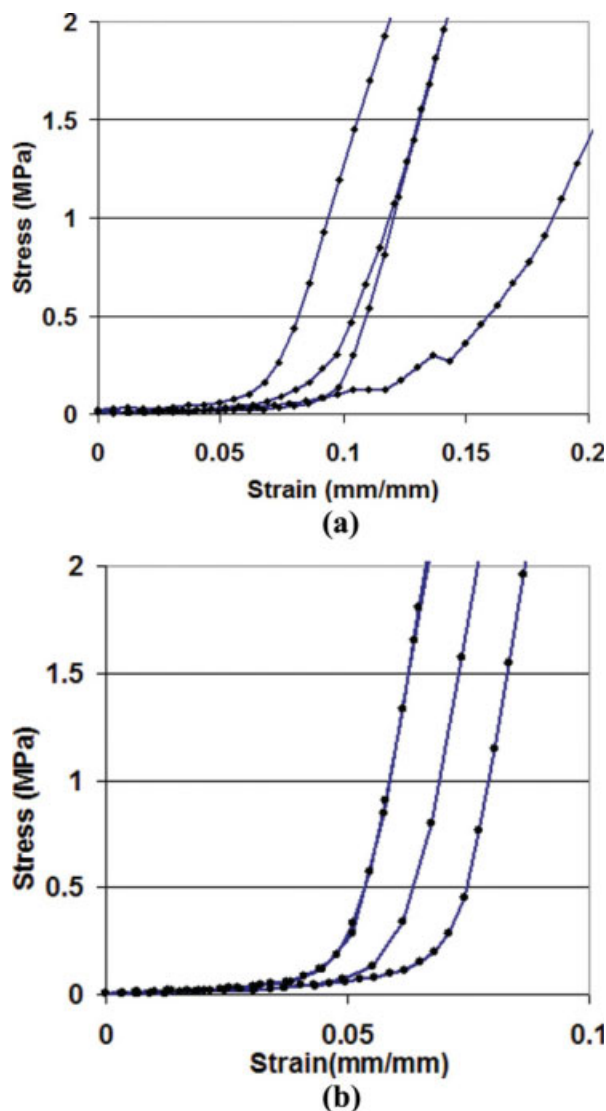
Figure 5 Initial strain region of stress-strain curves at 80°C and 100% relative humidity for (a) Nafion® and (b) Nafion®/titania composite membranes.

TABLE II
Mechanical Properties of Nafion® and Nafion®/Titania Membranes at 80°C and 100% Relative Humidity

	Modulus (MPa)	Length increase due to humidity change (%)	Strain at break (mm/mm)	Stress at break (MPa)
Nafion®/ titania	120.4 ± 7.1	5.7 ± 1.0	3.1 ± 0.2	24.1 ± 1.68
Nafion®	36.2 ± 7.2	10.0 ± 3.2	4.1 ± 0.4	20.8 ± 3.2

MPa for unmodified Nafion®. Table II summarizes the mechanical properties of the two materials. Thus, the incorporation of these sol-gel-derived structures not only enhances membrane modulus but also imparts better dimensional stability against humidity change which could be beneficial in enhancing the physical durability of membranes and in fuel cells.

Proton conductivity and fuel cell performance

The electrical impedance ($Z^* = Z' - Z''i$) behavior, in $-Z''$ vs. Z' graphs, of Nafion® and Nafion®/titania membranes in water at room temperature is shown in Figure 6 and the respective conductivities were computed to be 0.078 S.cm^{-1} and 0.033 S.cm^{-1}. Titania conductivity is less than half of that of Nafion®. Although the water uptake of the composite membrane is lower than that of Nafion® it may not be the sole reason for its low proton conductivity as both membranes were immersed in water. It is reasonable to think that the side chains become trapped in the inorganic quasi-networks. The strong acid groups at the ends of the side chains catalyze the sol-gel reaction of the already-reactive titanium
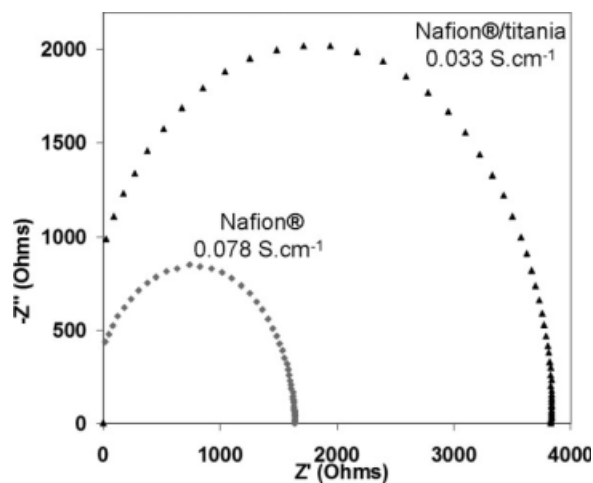
curve displacement is diagnostic of sample dimensional stability. After this, the curve has a profile typical of a ductile material and a modulus can be determined from the initial, displaced, linear region of the curve. The maximum strain up to the point when the stress begins to rise corresponds to the increase in sample length with respect to the initial dry length, i.e., the percent increase in sample length due to water uptake. The initial part of the curve for all samples is shown in Figure 5(a) and (b), as well. The Nafion®/titania membrane has better dimensional stability than that of Nafion® because the average percent increase in length for the composite membrane is 5 ± 1 % while that of Nafion® is 10 ± 3 %. Also, the average modulus computed from the stress-strain curves is 120 ± 7 MPa for the composite membrane but considerably lower at 36 ± 7

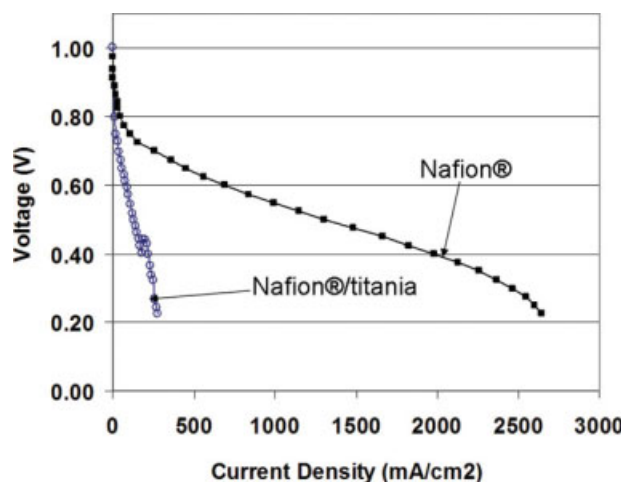**Figure 6** Impedance spectra of Nafion® and Nafion®/ titania composite membranes at room temperature in water.

Figure 7 Polarization curves for Nafion® and Nafion®/titania composite membranes at 80°C, Anode 100% RH, and cathode 50% RH.

iso-propoxide monomer so that branched titanate structures could rapidly form cages around the acid groups and shield them from being proton hopping sites. However, it was seen that there are changes in neither the EW nor the environment around these groups (according to the FTIR results) with titania incorporation. This suggests that the sulfonic acid groups are not blocked by the inorganic inclusions. However, if titanate structures are in intimate contact with side chains in the vicinity of the ether oxygens (as suggested by the FTIR results), the mobility of the side chains would be restricted, thereby accounting for the mechanical properties.

The decrease in conductivity could be due to a reduction in side chain mobility, proton migration tortuosity, and impeding interactions of protons with the titania nanostructures (e.g., accessible TiOH groups). The conductivity σ can, in general terms, be written as the product of the charge carrier density ρ and mobility μ. Because the charge carrier density, i.e., EW, is unaffected by the titanate modification, μ, and therefore σ could be diminished by the factors listed above.

Fuel cell performance

Although the primary focus of this work was to evaluate the mechanical durability of Nafion® as affected by titania modification, the fuel cell performance of this membrane was not optimized although initial results will be presented here. The polarization curves of the Nafion®/titania and Nafion® control membranes in the fuel cell are shown in Figure 7. The performance of the titania-incorporated Nafion® membrane is extremely poor compared with that of pure Nafion®. Based on low-

water uptake and low-proton conductivity, poor performance is not unexpected. To obtain better performance perhaps there should be enough mobility for the side chains to participate in proton transport or induce inorganic structures that allow the membrane to hydrate better.

Open circuit voltage decay

The OCV for Nafion®/titania and Nafion® MEAs measured for 20 h is shown in Figure 8. For the composite MEA, the OCV starts at 1.006 V whereas for the control sample it starts at 0.971 V. The fact that the starting value of OCV for Nafion®/titania is 3.6% higher than that of Nafion® could be attributed to better gas barrier properties. Incorporation of the inorganic component reduced fuel crossover and minimized voltage loss. This is further supported by the rate of decay of the OCV. In 20 h the OCV for Nafion® decreased by 0.091 V at a rate of 4.5 mV/h whereas for Nafion®/titania it decreased by 0.025 V at a rate of 1.2 mV/h. The voltage decay rate for pure Nafion® is 3.5 times higher than that of the Nafion®/titania composite membrane. Thus, incorporation of the inorganic quasi-network structures enhances membrane barrier properties and can increase cell performance by minimizing voltage loss associated with fuel crossover, although proton conductivity is still a problem.

Fluoride emission rate

The fluoride content of the effluent collected during the OCV study for both anode and cathode is shown in Figure 9. The FER for the Nafion®/titania MEA is at least an order of magnitude less than that of pure
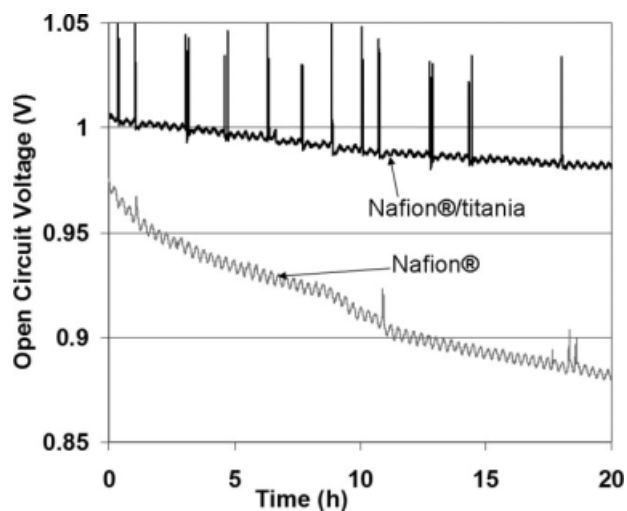

Figure 8 Open circuit voltage curves for Nafion® and Nafion®/titania composite membranes at 90°C and 30% relative humidity.
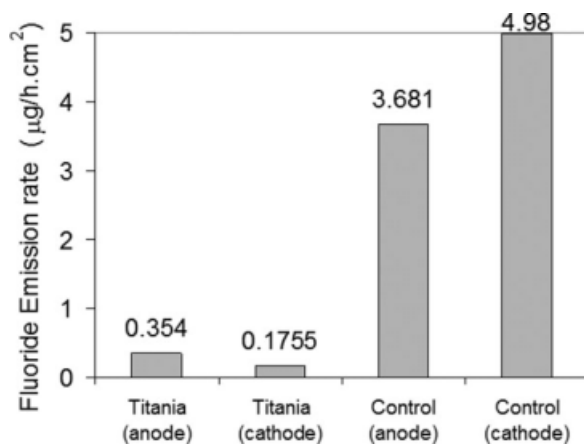
Figure 9 FERs of Nafion® and Nafion®/titania composite membranes for anode and cathode.

Nafion®. The FER test indicates a reduced rate of the chemical degradation of Nafion® affected by the titania component. This is again attributed to better gas barrier properties partly due to introduced tortuosity but perhaps also due to gas interactions with the inorganic nanostructures. Reduction in fuel crossover may have lowered the rate of hydrogen peroxide formation which could reduce the rate of membrane chemical degradation. By reducing fuel crossover one can not only reduce the voltage loss and increase cell efficiency but can also retard membrane degradation.

CONCLUSIONS

Incorporation of bonded titania quasi-networks in the polar domains of Nafion® via a membrane—in situ sol-gel process was confirmed using FTIR spectroscopy. Titration showed that the EW of Nafion® was unchanged after this incorporation. Mechanical analysis of contractile stress buildup during drying from a swollen state in a sample clamped at constant length demonstrated considerable Nafion® reinforcement by the titania structures that act to resist dimensional change. However, un-reinforced Nafion® failed in a way that reflects slippage of polymer chains through entanglements in uncrosslinked systems. These conclusions were supported by tensile stress vs. strain studies in which it was found that the composite membrane exhibited a larger initial modulus. However, while this modification enhanced membrane durability, the composite membrane showed lower water uptake, lower proton conductivity and poor cell performance, although these initial studies were primarily directed toward understanding mechanical durability.

OCV decay studies showed that incorporation of the inorganic component reduced fuel crossover and minimized voltage loss, attributed to better gas bar-

rier properties. FER testing indicated a reduced rate of chemical degradation of Nafion® affected by the titania component which is attributed to better gas barrier properties, perhaps due to introduced gas diffusion pathway tortuosity.

Some of these phenonomena can be explained in terms of side chains that become entrapped in the evolving inorganic quasi-networks during the in situ sol-gel process. The mechanical studies infer strong interactions between, or mixing of, the organic and inorganic components. Increased cohesion in the cluster regions would also diminish water swelling. But the fact that the EW of the membrane is unchanged, as well as the invariance of the symmetric and asymmetric SO_3^- group infrared bands after the inorganic incorporation, suggests that these groups are not blocked and perhaps protruding from the titania structures.

A reason for the poor fuel cell performance is likely the high volume of titania in the polar domains. If the majority of hydrophilic volume is occupied by titania quasi-networks so as to constrain the side chains, their mobility would be restricted in a way that would diminish proton hopping kinetics and more proton hopping tortuosity would be introduced. As stated, these were meant as model studies with a focus on mechanical durability. Inorganic modification that improves membrane performance will be sought. Modifications that could be pursued would be manipulating the considerable sol-gel reaction variables (solvent type, pH, temperature, catalysts, co-condensation with other metal alkoxides) to have more hydrophilic TiOH groups as well as cause more hyperbranched particles.

Nonetheless, incorporation of the inorganic quasi-network particles reduces the physical and chemical degradation of the Nafion® membrane which, assumedly, could withstand physical stresses due to humidity and temperature changes. Moreover, improved barrier properties have reduced chemical degradation and voltage loss due to reduced fuel crossover.

References

1. Mauritz, K. A.; Moore, R. B. Chem Rev 2004, 104, 4535.
2. Borup, R.; Meyers, J.; Pivovar, B.; Kim Yu, S.; Mukundan, R.; Garland, N.; Myers, D.; Wilson, M.; Garzon, F.; Wood, D.; Zelenay, P.; More, K.; Stroh, K.; Zawodzinski, T.; Boncella, J.; McGrath James, E.; Inaba, M.; Miyatake, K.; Hori, M.; Ota, K.; Ogumi, Z.; Miyata, S.; Nishikata, A.; Siroma, Z.; Uchimoto, Y.; Yasuda, K.; Kimijima, K.-I.; Iwashita, N. Chem Rev 2007, 107, 3904.
3. Aoki, M.; Uchida, H.; Watanabe, M. Electrochem Commun 2006, 8, 1509.

4. Escobedo, G. Fuel Cells Durability, 1st ed.; Knowledge Press; Brookline, MA, 2006; p 83.

5. Zhou, C.; Guerra, M. A.; Qiu, Z.-M.; Zawodzinski, T. A.; Schiraldi, D. A. Macromolecules 2007, 40, 8695.

6. Schiraldi, D. A.; Zhou, C.; Reinardy, A.; Zawodzinsk, T. A. Prepr Symp—Am Chem Soc, Div Fuel Chem 2008, 53, 821.

7. Antoine, O.; Durand, R. J Appl Electrochem 2000, 30, 839.

8. Liu, W.; Crum, M. ECS Trans 2006, 3, 531.

9. Mauritz, K. A.; Hassan, M. K. Polym Rev 2007, 47, 543.

10. Deng, Q.; Moore, R. B.; Mauritz, K. A. Chem Mater 1995, 7, 2259.

11. Falk, M. ACS Symp Ser 1982, 180, 139.

12. Siuzdak, D. A.; Start, P. R.; Mauritz, K. A. J Polym Sci Part B: Polym Phys 2002, 41, 11.

13. Mauritz, K. A.; Jones, C. K. J Appl Polym Sci 1990, 40, 1401.

14. Bradley, D. C.; Mehrotra, R. C.; Gaur, D. P. Met Alkoxides, Academic; London, England, 1978, p 118.

15. Samms, S. R.; Wasmus, S.; Savinell, R. F. J Electrochem Soc 1996, 143, 1498.

16. Wilkie, C. A.; Thomsen, J. R.; Mittleman, M. L. J Appl Polym Sci 1991, 42, 901.

17. Ferry, J. D.Viscoelastic Properties of Polymers, 3rd ed.; Wiley: New York, 1961.